



Published in final edited form as:

Connect Tissue Res. 2017 ; 58(3-4): 259–270. doi:10.1080/03008207.2016.1268604.

Relevance of meniscal cell regional phenotype to tissue engineering

Shawn P. Grogan,

Shiley Center for Orthopaedic Research and Education at Scripps Clinic, La Jolla, CA

Chantal Pauli,

Department of Molecular and Experimental Medicine, The Scripps Research Institute, La Jolla, CA

Martin K. Lotz, and

Department of Molecular and Experimental Medicine, The Scripps Research Institute, La Jolla, CA

Darryl D. D'Lima

Shiley Center for Orthopaedic Research and Education at Scripps Clinic, La Jolla, CA

Abstract

Purpose—Meniscus contains heterogeneous populations of cells that have not been fully characterized. Cell phenotype is often lost during culture; however, culture expansion is typically required for tissue engineering. We examined and compared cell surface molecule expression levels on human meniscus cells from the vascular and avascular regions and articular chondrocytes while documenting changes during culture-induced dedifferentiation.

Materials and Methods—Expression of 16 different surface molecules were examined by flow cytometry after monolayer culture for 24 h, 1 week, and 2 weeks. Menisci were also immunostained to document the spatial distributions of selected surface molecules.

Results—Meniscus cells and chondrocytes exhibited several similarities in surface molecule profiles with dynamic changes during culture. A greater percentage of meniscal cells were positive for CD14, CD26, CD49c, and CD49f compared to articular chondrocytes. Initially, more meniscal cells from the vascular region were positive for CD90 compared to cells from the avascular region or chondrocytes. Cells from the vascular region also expressed higher levels of CD166 and CD271 compared to cells from the avascular region. CD90, CD166, and CD271-positive cells were predominately perivascular in location. However, CD166-positive cells were also located in the superficial layer and in the adjacent synovial and adipose tissue.

Conclusions—These surface marker profiles provide a target phenotype for differentiation of progenitors in tissue engineering. The spatial location of progenitor cells in meniscus is consistent

Address correspondence to: Darryl D. D'Lima (MD, PhD), Shiley Center for Orthopaedic Research and Education at Scripps Clinic, 11025 North Torrey Pines Road, Suite 200, La Jolla, CA 92037, Tel 858 332 0166; Fax 858 332 0669, ddlima@scripps.edu.

Declaration of interest

The authors report no conflicts of interest. The authors alone are responsible for the content and writing of the article.

with higher regenerative capacity of the vascular region, while the surface progenitor subpopulations have potential to be utilized in tears created in the avascular region.

Keywords

Meniscus; Articular cartilage; Cell phenotype; Dedifferentiation; Flow cytometry

Introduction

The menisci play an important role in the complex biomechanics of the knee joint by providing joint lubrication, joint stability, joint congruity, and transmitting load (1, 2). Damaged or degenerated meniscus leads to overall knee joint destabilization and inappropriate loads on cartilage contributing to the development of osteoarthritis (OA) (3–5).

Partial or total meniscectomy can alleviate pain and joint function temporarily; however, the altered loading dynamics leads to degeneration (6), with all patients developing OA on average 14 years following intervention (7, 8). Tears located in the vascular region of meniscus sometimes heal due to the higher regenerative potential (9–11), most likely due to the existing blood supply and the possibility of progenitors located in this region (12). On the other hand, avascular meniscus tissue tears have little to no repair capacity and with limited options for repair. Tears and damage that span both regions are equally difficult to repair (13–16).

Surgical interventions to repair meniscus have included various sutures and natural or synthetic implants, yet these methods have not led to consistent outcomes (2, 17). Cell-based therapies represent an alternative approach to repair meniscus tears (18, 19) or for engineering meniscus implants (1, 20). However, our present knowledge of heterogeneous meniscus cell populations that inhabit and maintain this complex tissue is incomplete.

There are at least 3 cell populations that reside in the human meniscus. The main cell type in the inner and middle part of the meniscus (avascular region) has been termed the fibrochondrocyte (2). Fibrochondrocytes display fibrous and cartilaginous characteristics as a consequence of their chondrocytic appearance (round or oval shape and situated in well-formed lacunae) and the synthesis of fibrocartilage matrix (consisting mainly of collagen type I, with lower quantities of collagen type II and aggrecan) (21, 22).

The outer region of the meniscus is vascular with dense connective tissue consisting predominately of collagen type I and is mainly populated by fibroblast-like cells with long cell extensions. At the very surface (superficial zone of meniscus), is a cell type without cell extensions and apparently analogous to the superficial zone (SZ) of articular cartilage. Like the superficial zone of cartilage, the superficial zone of the meniscus may harbor progenitor cells (23–25). Ghadially et al. indicated similarity between the cells of the meniscal superficial zone to those of chondrocytes in the SZ of articular cartilage and the cells of the inner regions of the meniscus to the chondrocytes of the middle and deep zones of articular cartilage (26).

In cell-based tissue engineering, expansion of cells in culture to achieve appropriate cell numbers is a common requirement. During expansion, the cells undergo de-differentiation, as typically shown in chondrocytes with the classic shift in collagen type II and aggrecan expression to collagen type I and versican expression (27–31), as well as changes in several cell surface molecules including a shift in the ratio of CD14/CD90 (30). Similar to articular chondrocytes, isolated meniscus cells also appear to undergo monolayer culture-induced dedifferentiation with a loss of collagen type II, COMP and with increased collagen type I production (32, 33). However, there is a lack of information regarding the surface marker expression of meniscus cells isolated from different regions and the changes induced by monolayer culture. Elucidating the phenotype of the meniscus cell types during the process of isolation, expansion, and redifferentiation is very relevant to cell-based meniscus tissue engineering.

We therefore aimed i) to analyze dynamic changes in cell surface molecule expression in human meniscus cells during culture-induced dedifferentiation and in comparison to human chondrocytes and ii) to identify potential progenitor cell populations within human meniscus.

Materials and methods

Human meniscus and cartilage procurement

Normal human articular cartilage and menisci (medial and lateral) were obtained from tissue banks (after Scripps Institutional Review Board approval). Normal menisci were selected using the macroscopic and histologic grading system by Pauli et al. (34) and normal cartilage were selected using Mankin grades 0–1. Menisci from 10 donors (mean age: 54.3 ± 26.0; age range: 15–90 years; 3 females, 7 males) and cartilage from 5 donors (mean age: 44.2 ± 20.7; age range: 22–68 years; 2 females, 5 males) were harvested. Representative portions of menisci were processed for histology as detailed below. To separate the vascular and avascular regions, the inner (avascular region) and outer (vascular region) one-third were harvested; the middle third (red-white zone) was discarded. Articular cartilage and meniscus tissues were digested using collagenase (2 mg/ml; C5138, Sigma-Aldrich, St. Louis, MO) in Dulbecco's Modified Eagle Medium (DMEM) (Mediatech Inc, Manassas, VA) and 1% Penicillin-Streptomycin-Gentamycin (Life Technologies, Carlsbad, CA) for 5 to 6 h. The digested tissues were filtered through 100 µm cell strainers (BD Biosciences, San Jose, CA) and were seeded in DMEM (Mediatech) supplemented with 10% calf serum (Omega Scientific Inc. Tarzana, CA) and 1% Penicillin-Streptomycin-Gentamycin (Life Technologies). Cells were maintained in monolayer culture. Cells from each donor were seeded at a density of 15,000 cells per cm². The cells were never passaged, but were harvested after culture for 24h, 1 week and 2 weeks. At each time point, the cells were detached with Accutase (Innovative Cell Technologies, San Diego, CA), frozen in calf serum with 10% DMSO, and stored in liquid nitrogen until needed for flow cytometry. An overview of the experimental flow is provided in Supplementary Figure 1.

Flow cytometry

Cryopreserved cells were thawed and washed in phosphate-buffered saline (PBS), were counted and suspended in FACS buffer consisting of Hank's Balanced Salt Solution (HBSS; Gibco) and 0.1% bovine serum albumin (BSA; Sigma), and were maintained on ice. A total of 16 surface molecules were selected to document changes due to cell culture-induced dedifferentiation mainly based on the panel utilized by Diaz-Romero et al. (35). These molecules included CD14, CD26, CD44, CD49a, CD49c, CD49e, CD49f, CD54, CD90, CD95, CD105, CD106, CD140a, CD151, CD166, and CD271. Supplementary Table 1 lists the biological relevance and the source of the CD molecules. Matching isotype controls were used to detect nonspecific staining and background signal. To assess live cell fluorescence signals, 7-Aminoactinomycin D (7-AAD; ThermoFisher Scientific) was used to monitor cell viability. The percentage positive calculations and the geometric mean fluorescence intensity (MFI) data were based on the background signal gated at 1%.

Histology processing

Immediately after harvesting, medial human menisci from knee donors were fixed in Z-Fix (Anatech, Ltd. Battle Creek, MI) as previously described (34). After dehydration with alcohol, paraffin, and infiltration with paraffin, all the tissue samples were embedded in paraffin in the sagittal planes (cross section/triangle). Microtome sections cut at 4 μ m were stained with Safranin O/Fast Green or prepared for immunohistochemistry.

Immunohistochemistry

To identify progenitor cell subpopulations within native meniscus tissue, immunostaining for CD90 (Thymocyte antigen 1; (THY-1), CD271 (Low-affinity nerve growth factor receptor, LNGFR) and CD166 (Activated leukocyte cell-adhesion molecule (ALCAM)) were performed on paraffin-embedded human menisci from 10 donors.

The antibody retrieval methods were unique for each antibody as outlined below. The secondary antibody and color development were the same for each CD molecule examined.

To detect CD90 (THY-1), deparaffinized sections were incubated in 0.1% Triton™ in PBS for 5 minutes and then were blocked in 10% normal goat serum for 30 minutes at room temperature. A rabbit monoclonal antibody against human CD90 (Abcam, Cambridge, MA) was used at 1 μ g/ml in 0.1% Triton in PBS and was incubated overnight at 4°C. A rabbit IgG at 1 μ g/ml was used as a negative control.

For CD166 (ALCAM) deparaffinized sections were incubated with 3% H₂O₂ in methanol for 10 minutes at room temperature, followed by heating sections in citric acid buffer (pH 6.0) to 90°C for 14 minutes in a steamer. Each section was blocked in 10% normal goat serum for 30 minutes at room temperature. A rabbit polyclonal (clone H-108; Santa Cruz) was used at 1 μ g/ml and rabbit IgG was used to monitor nonspecific background staining.

The presence of CD271 in meniscus was tested using a rabbit anti-CD271 antibody (Proteintech Group, Inc. Chicago, IL). After deparaffinization, the sections were placed into a citric acid buffer (pH 6.0), were microwaved at 70% power (900 watt) 2x2 minutes, and were permitted to cool to room temperature. After rinsing in Tris-buffer saline with 0.05%

Tween 20 (TBST) twice for 5 minutes, the sections were incubated in 3% H₂O₂ in methanol for 30 minutes at room temperature. The primary antibody (2 µg/ml) was incubated with the tissues overnight at 4°C. The slides were then washed twice in TBST.

Following primary antibody incubations overnight for either CD90, CD166, or CD271 the sections were washed in PBS and a biotinylated anti-rabbit secondary antibody was used (1 µg/ml) and were incubated in a humid container at room temperature for 1 h. The VECTASTAIN ABC-AP KIT (standard) (AK-5000; Vector Laboratories) was used for color visualization (red). Some sections were counterstained with hematoxylin to stain nuclei (blue). All sections were dehydrated in ethanol and propar and were mounted with a coverslip with Refrax mounting medium (Anatech).

Statistical analysis

Comparisons between percentage positive fluorescence signal and MFI for a given surface marker and cell source were first analyzed using the non-parametric Kruskal-Wallis test, followed by pair-wise comparisons using the Dwass-Steel-Critchlow-Fligner test. A p-value of 0.05 or less was considered significant.

Results

Surface molecule expression profiles of meniscus cells and chondrocytes show similar dynamic temporal changes during culture

Table 1 presents a summary of the surface molecule profiles for avascular meniscal cells, vascular meniscal cells and articular chondrocytes at 24 h, 1 week, and 2 weeks. For the majority of cell types, the percentage of cells expressing a given surface molecule significantly ($p < 0.05$) increased over time in culture in comparison to the 24 h time point (Table 1 and Figure 1). Fold change for both percentage and mean fluorescent intensity relative to 24 h data are provided in Tables 2 and 3, respectively.

Significant differences in surface molecule expression levels between populations studied

CD14—The percentage of CD14-positive human chondrocytes was higher than that of meniscal cells at 24 h (Figures 1 and 2A, $p < 0.03$). However, the percentage of CD14-positive human chondrocytes reduced significantly after 2 weeks in culture (Table 1 Figures 1 and 2A, $p < 0.03$), while that of meniscal cells did not.

CD90—Overall, CD90 (Thy-1) levels were low in all 3 cell types at 24 h, yet significantly increased greater than 6-fold after 2 weeks in culture (Figures 1 and 2B and Table 2). At 24 h a significantly higher ($p < 0.05$) percentage of CD90-positive cells were detected in the vascular meniscus group compared to avascular meniscus and chondrocytes (Figures 1 and 2B; Table 1). Representative histograms of CD14 and CD90 displayed in Figure 2 show the shifts on staining over time.

CD26—At 24 h the percentage expression of CD26 (peptidase IV) was significantly lower in articular chondrocytes (24%) compared to either avascular (48%) or vascular (58%) meniscus cells (Figure 1C, $p < 0.01$).

CD 49c—Vascular meniscus cells at 24 h were around 30% positive for CD49c (integrin α 3 subunit), which was significantly higher than chondrocytes (8%) at the same time point (Figure 1D, $p < 0.04$).

CD271—CD271 levels were low ($2.5 \pm 3.0\%$; Table 1) and decreased over time in culture to less than 1%.

Vascular regions and the surface of meniscus may harbor progenitor cells

Progenitor cells express CD90, CD166, and CD271 (36). To determine the spatial localization of potential progenitors within meniscus tissues, sagittal sections of human meniscus tissues were stained with antibodies specific for CD90, CD166 and CD271. Positive staining was predominately identified in cells that surrounded blood vessels (Figures 3A–3C). Cells staining positive for CD166 (ALCAM) were also found in 2 distinct locations in the meniscus: associated with blood vessels in the vascular region and in the superficial zone of meniscus, which were negative for both CD90 and CD271 (Figure 4). CD166-positive cells were found to line the entire length of the superficial zone of the menisci as shown in the representative image in Figure 4C. CD166-positive cells were also found in the adjacent synovial tissue.

Discussion

The human meniscus contains heterogeneous populations of cells, which have yet to be completely characterized. Surface molecule profiles are commonly used to identify cell phenotypes. Cell isolation from tissues and cell culture often induces distinct changes in cell phenotype, which are reflected in corresponding changes in surface molecule profiles. In this study, we observed that the surface molecule profiles of meniscus cells from vascular or avascular regions resembled those of chondrocytes with significantly dynamic changes during culture. Some of the similarities found in surface molecule expression were indicative of the overlapping characteristics and the fibrocartilaginous nature of meniscal tissue. Despite several similarities, distinct differences were noted between cells from the meniscus and those from articular cartilage, as well as between meniscus cells derived from regions based on vascularity. The major differences between meniscus and chondrocytes are the expression levels of CD14 (LPS-receptor), CD49c (integrin alpha 3 subunit) and CD26 (Dipeptidyl peptidase IV). The higher frequency of progenitor-like cell populations in the vascular region was the most distinctive difference in comparison with the avascular region.

The surface marker profiles in meniscus cells and chondrocytes during monolayer-induced cell dedifferentiation provided several clues toward maintenance of meniscus phenotype. In particular, CD90 or THY-1 is an interesting molecule on many levels. This glycosylphosphatidylinositol-linked protein is involved in many processes including cell-cell and cell-matrix interactions (37), cytoskeleton changes, proliferation, cellular adhesion, proliferation, survival, and growth factor/cytokine responses (38–40). We observed a higher percentage of CD90-positive cells from vascular region of the meniscus, which is consistent with the more fibroblast-like phenotype. The expression level of CD90 during dedifferentiation increased, as all cells (chondrocytes and meniscus cells) become more fibroblast-like in culture. Surface expression of CD90 is known to inhibit src-kinase

activation leading to increased stress fiber formation and focal adhesion complexes (38). The shift in collagen subtype from type II to type I during chondrocyte dedifferentiation was reflected in the inverse relationship between expression of CD90 and CD14 (30). In dedifferentiating chondrocytes, as CD90 levels increased, the surface expression of CD14 decreased. However, in meniscus cells, CD14 levels did not change significantly over time in culture. CD14 is part of the lipopolysaccharide (LPS) complex and is a toll-like receptor (TLR) signaling pathway that interacts with heparan and may be involved in breakdown of extracellular matrix (ECM) molecules such as heparan sulfate (41). More importantly, signaling through CD14/TLR4 may maintain an undifferentiated progenitor phenotype (42, 43). Overall, the CD90 and CD14 expression profiles in meniscus cells were closer to that of a dedifferentiated chondrocyte. In general, a higher CD90 to support stress fiber formation and a lower CD14 expression may reduce ECM turnover and may aid in maintaining the meniscus phenotype.

Integrins are also likely to play a role in maintaining meniscus differentiation status. Integrins are arranged as heterodimers of α and β units, which are single-pass transmembrane adhesion proteins that interface between the surrounding ECM (44) and the actin cytoskeleton (45). These interactions transmit mechanical force for cellular signaling to regulate many cellular responses such as migration, survival, motility, and differentiation (46–48). With regard to phenotype regulation, integrins interact with the cytoskeleton, which regulates chondrocyte phenotype (49) involving various integrin signaling pathways such as integrin-linked kinase (ILK) focal adhesion kinase (FAK), mitogen-activated protein kinases (MAPK) and members of the Rho GTPases family (50).

Little is known about the role of integrins and integrin signaling pathways in meniscal cells. In this present study, we observed a significantly higher expression of integrin $\alpha 3$ (CD49c) in meniscus cells isolated from the vascular region compared to chondrocytes. Integrin $\alpha 3$ is involved in complexes that orchestrate focal adhesion and in actin stress fiber formation (51). Such an association is consistent with the previously discussed association with CD90/CD14 and stress fiber formation and the vascular meniscus fibroblast-like phenotype. Extracellular ligands for integrins include laminins, fibronectin, collagens, or RGD-containing proteins (52–54). The $\alpha 3\beta 1$ -integrins play an important role in modulating the assembly of pericellular matrices in the kidney (54). Interestingly, $\alpha 3\beta 1$ -integrins can alter MMP2 activity by binding to laminin (52), which may be important in modulating avascular meniscus tissue homeostasis. Regional differences in ECM composition in the meniscus may aid in understanding the interactions between these different surface molecules to maintaining healthy meniscus tissue.

Another possible contributor of promoting or sustaining the meniscus phenotype is CD26 or Dipeptidyl peptidase IV (DPP4). Meniscus cells were significantly more positive for CD26 at 24 h compared to chondrocytes. One of the biological roles of this ectoenzyme includes the regulation of extracellular adenosine levels, which modulates chondrogenesis. Increased adenosine levels promote cartilage differentiation, COL2A1 gene expression, and ECM synthesis (55–57). Increased CD26 expression is accompanied by increased levels of Adenosine deaminase (ADA) (58, 59), which leads to ecto-ADA and degradation of adenosine (60). It was postulated that the increase in CD26 expression in cultured

chondrocytes may be related to reduction in chondrogenic capacity with increased passage (30). In the meniscus, higher levels of CD26 may be another mechanism to maintain a more fibroblast meniscus phenotype.

The FAS receptor (CD95) was significantly upregulated in all cell types examined by the second week in culture: approximately 50% of meniscus cells and 40% of chondrocytes were positive for CD95. Typically, an increase in CD95 levels may be expected to increase the potential for signaling a cytotoxic effect by inducing apoptosis (61, 62). However, CD95 can also promote cell proliferation and migration in various cell types including fibroblasts (63, 64), and liver (65), and can induce neurite outgrowth and accelerate nerve regeneration after injury (66). Increased FAS enhances survival of neural progenitor cells without increased proliferation (67). It remains to be determined whether CD95 in meniscal cells is an important regulator of cell proliferation or survival during monolayer expansion.

Overall, vascular meniscus cells had higher levels of progenitor cell molecules including CD90 (THY-1), CD166 (ALCAM), and CD271 (LNGFR) compared to avascular cells and the immune-localization studies confirm positive signals for these molecules, especially in the perivascular regions. Identification of CD166-positive cells in the surface layers of the meniscus in our current study is consistent with previous reports indicating the presence of stem or progenitor cells in this area (23–25). The expression of CD166 suggests that these cells could be progenitors. However, presence of other markers, e.g., CD29, CD36, and CD73 (68), and functional assays are required for more definitive identification. The presence of progenitor cells would appear to be in conflict with the capacity of the avascular region to self-heal (14–16). Meniscus progenitors in normal meniscal tissue are likely quiescent, but cells positive for several stem cell markers including CD105, CD106 and STRO-1 emerge from and migrate into diseased or disrupted tissues (25). Although the inner bulk tissue of the avascular region lacked identifiable progenitor populations, the presence of progenitors on the surface of the meniscus opens the possibility of developing methods to better characterize, stimulate, and utilize these cells. Studies are needed to determine whether these progenitors have the capacity to heal tears or lesions. For instance, the emergence of the α SMA expression in torn menisci, reported by Declercq et al. (23), may reflect mobilization of the same CD166-positive population that we detected in the surface of normal menisci. Our immunostaining revealed many CD166 positive cells in the synovial and adipose tissues adjacent to the meniscus. The notion that the meniscus cell-surface population may originate from the synovium and surrounding tissues warrants further investigation, as these cells may have regenerative properties relevant to meniscus tissue engineering.

While the shift in ECM molecule expression and surface molecules is well documented in chondrocytes, there are no such definitive ECM molecules for meniscus. Similar changes in cell morphology during culture in both chondrocytes and meniscus together with the very similar changes in many surface molecules in both cell types indicate that the meniscus cells are converging to a similar dedifferentiated state. Our ongoing work aims to identify specific meniscus ECM molecules that are altered due to culture and to identify evidence of markers of meniscus dedifferentiation. In the context of tissue engineering, it may be useful to follow changes in these surface molecule profiles during redifferentiation, which is dependent on

whether culture expanded (dedifferentiated) meniscus cells show a similar capacity as chondrocytes to redifferentiate in 3D cultures. Using these surface molecule profiles may also aid in further refining conditions needed for meniscus tissue formation.

Overall, only 10 meniscus donors were examined in this study, which also spanned a large age range (15 to 90 years). Although the signatures were remarkably similar between ages, it would make sense to screen more donors from matching aged cohorts to determine whether aging influences surface molecule expression. The present data indicates that all cell populations examined lack clonal populations, yet a single cell clone culture approach would be needed to detect true clonal populations. An expansion of more surface molecules would also be needed to increase the detection of clonal populations, including more in depth analysis of progenitor cells in meniscus.

In conclusion, the surface molecule profile of human meniscus cells changed significantly over time in monolayer culture, with several notable differences relative to the profile of articular chondrocytes. These differences appear to be related to important phenotypical distinctions between cells of meniscus and cartilage origin. Cells from the vascular region of the meniscus and cells at the surface expressed markers indicative of progenitor cells. The dynamic changes in surface molecule profiles during culture provide a useful model to study meniscus cell dedifferentiation and redifferentiation as well as a target phenotype for differentiation of progenitors and stem cells for tissue engineering.

Supplementary Material

Refer to Web version on PubMed Central for supplementary material.

Acknowledgments

We are grateful for the technical support by Sujata Sovani, Yukio Akasaki, Emily Lee, and Tammy Lee (immunostainings) and by Judy Blake (Copyediting).

Funding

The National Institutes of Health (P01 AG007996), the Shaffer Family Foundation, and Donald and Darlene Shiley provided funding for this project.

References

1. Guo W, Liu S, Zhu Y, Yu C, Lu S, Yuan M, Gao Y, Huang J, Yuan Z, Peng J, Wang A, Wang Y, Chen J, Zhang L, Sui X, Xu W, Guo Q. Advances and prospects in tissue-engineered meniscal scaffolds for meniscus regeneration. *Stem Cells Int.* 2015; 2015:517520. [PubMed: 26199629]
2. Makris EA, Hadidi P, Athanasiou KA. The knee meniscus: Structure-function, pathophysiology, current repair techniques, and prospects for regeneration. *Biomaterials.* 2011; 32:7411–7431. [PubMed: 21764438]
3. McDermott ID, Amis AA. The consequences of meniscectomy. *J Bone Joint Surg Br.* 2006; 88:1549–1556. [PubMed: 17159163]
4. Mononen ME, Jurvelin JS, Korhonen RK. Effects of radial tears and partial meniscectomy of lateral meniscus on the knee joint mechanics during the stance phase of the gait cycle--a 3d finite element study. *J Orthop Res.* 2013; 31:1208–1217. [PubMed: 23572353]

5. Moore AC, Burris DL. Tribological and material properties for cartilage of and throughout the bovine stifle: Support for the altered joint kinematics hypothesis of osteoarthritis. *Osteoarthritis Cartilage*. 2015; 23:161–169. [PubMed: 25281916]
6. Blackmore SA, McGee AW Jr, Gladstone JN, Strauss EJ, Davidson PA, Jazrawi LM. The management of meniscal pathology: From partial meniscectomy to transplantation. *Instr Course Lect*. 2015; 64:511–520. [PubMed: 25745934]
7. Englund M, Roos EM, Roos HP, Lohmander LS. Patient-relevant outcomes fourteen years after meniscectomy: Influence of type of meniscal tear and size of resection. *Rheumatology (Oxford)*. 2001; 40:631–639. [PubMed: 11426019]
8. Lohmander LS, Englund PM, Dahl LL, Roos EM. The long-term consequence of anterior cruciate ligament and meniscus injuries: Osteoarthritis. *Am J Sports Med*. 2007; 35:1756–1769. [PubMed: 17761605]
9. Krych AJ, McIntosh AL, Voll AE, Stuart MJ, Dahm DL. Arthroscopic repair of isolated meniscal tears in patients 18 years and younger. *Am J Sports Med*. 2008; 36:1283–1289. [PubMed: 18319351]
10. Longo UG, Campi S, Romeo G, Spiezia F, Maffulli N, Denaro V. Biological strategies to enhance healing of the avascular area of the meniscus. *Stem Cells Int*. 2012; 2012:528359. [PubMed: 22220179]
11. McCarty EC, Marx RG, DeHaven KE. Meniscus repair: Considerations in treatment and update of clinical results. *Clin Orthop Relat Res*. 2002; 402:122–134.
12. Osawa A, Harner CD, Gharaibeh B, Matsumoto T, Mifune Y, Kopf S, Ingham SJ, Schreiber V, Usas A, Huard J. The use of blood vessel-derived stem cells for meniscal regeneration and repair. *Med Sci Sports Exerc*. 2013; 45:813–823. [PubMed: 23247715]
13. Cooper DE, Arnoczky SP, Warren RF. Meniscal repair. *Clin Sports Med*. 1991; 10:529–548. [PubMed: 1868558]
14. Greis PE, Holmstrom MC, Bardana DD, Burks RT. Meniscal injury: Ii. Management. *J Am Acad Orthop Surg*. 2002; 10:177–187. [PubMed: 12041939]
15. Inoue T, Taguchi T, Imade S, Kumahashi N, Uchio Y. Effectiveness and biocompatibility of a novel biological adhesive application for repair of meniscal tear on the avascular zone. *Sci Technol Adv Mater*. 2012; 13:064219–064224. [PubMed: 27877546]
16. Mordecai SC, Al-Hadithy N, Ware HE, Gupte CM. Treatment of meniscal tears: An evidence based approach. *World J Orthop*. 2014; 5:233–241. [PubMed: 25035825]
17. Liu C, Toma IC, Mastrogiacomo M, Krettek C, von Lewinski G, Jagodzinski M. Meniscus reconstruction: Today's achievements and premises for the future. *Arch Orthop Trauma Surg*. 2013; 133:95–109. [PubMed: 23076654]
18. Cucchiari M, McNulty AL, Mauck RL, Setton LA, Guilak F, Madry H. Advances in combining gene therapy with cell and tissue engineering-based approaches to enhance healing of the meniscus. *Osteoarthritis Cartilage*. 2016
19. Yu H, Adesida AB, Jomha NM. Meniscus repair using mesenchymal stem cells - a comprehensive review. *Stem Cell Res Ther*. 2015; 6:86. [PubMed: 25925426]
20. Ballyns JJ, Wright TM, Bonassar LJ. Effect of media mixing on ECM assembly and mechanical properties of anatomically-shaped tissue engineered meniscus. *Biomaterials*. 2010; 31:6756–6763. [PubMed: 20541796]
21. McDevitt CA, Mukherjee S, Kambic H, Parker R. Emerging concepts of the cell biology of the meniscus. *Curr Opin Orthop*. 2002; 13:345–350.
22. Melrose J, Smith S, Cake M, Read R, Whitelock J. Comparative spatial and temporal localisation of perlecan, aggrecan and type i, ii and iv collagen in the ovine meniscus: An ageing study. *Histochem Cell Biol*. 2005; 124:225–235. [PubMed: 16028067]
23. Declercq HA, Forsyth RG, Verbruggen A, Verdonk R, Cornelissen MJ, Verdonk PC. Cd34 and sma expression of superficial zone cells in the normal and pathological human meniscus. *J Orthop Res*. 2012; 30:800–808. [PubMed: 22025365]
24. Lin BY, Richmond JC, Spector M. Contractile actin expression in torn human menisci. *Wound Repair Regen*. 2002; 10:259–266. [PubMed: 12191009]

25. Muhammad H, Schminke B, Bode C, Roth M, Albert J, von der Heyde S, Rosen V, Miosge N. Human migratory meniscus progenitor cells are controlled via the *tgf-beta* pathway. *Stem Cell Reports*. 2014; 3:789–803. [PubMed: 25418724]
26. Ghadially FN, Lalonde JM, Wedge JH. Ultrastructure of normal and torn menisci of the human knee joint. *J Anat*. 1983; 136:773–791. [PubMed: 6688412]
27. Benya PD, Padilla SR, Nimni ME. Independent regulation of collagen types by chondrocytes during the loss of differentiated function in culture. *Cell*. 1978; 15:1313–1321. [PubMed: 729001]
28. Benya PD, Shaffer JD. Dedifferentiated chondrocytes reexpress the differentiated collagen phenotype when cultured in agarose gels. *Cell*. 1982; 30:215–224. [PubMed: 7127471]
29. Gay S, Muller PK, Lemmen C, Remberger K, Matzen K, Kuhn K. Immunohistological study on collagen in cartilage-bone metamorphosis and degenerative osteoarthritis. *Klin Wochenschr*. 1976; 54:969–976. [PubMed: 790012]
30. Diaz-Romero J, Nestic D, Grogan SP, Heini P, Mainil-Varlet P. Immunophenotypic changes of human articular chondrocytes during monolayer culture reflect bona fide dedifferentiation rather than amplification of progenitor cells. *J Cell Physiol*. 2008; 214:75–83. [PubMed: 17559082]
31. Martin I, Jakob M, Schafer D, Dick W, Spagnoli G, Heberer M. Quantitative analysis of gene expression in human articular cartilage from normal and osteoarthritic joints. *Osteoarthritis Cartilage*. 2001; 9:112–118. [PubMed: 11237658]
32. Gunja NJ, Athanasiou KA. Passage and reversal effects on gene expression of bovine meniscal fibrochondrocytes. *Arthritis Res Ther*. 2007; 9:R93. [PubMed: 17854486]
33. Nakata K, Shino K, Hamada M, Mae T, Miyama T, Shinjo H, Horibe S, Tada K, Ochi T, Yoshikawa H. Human meniscus cell: Characterization of the primary culture and use for tissue engineering. *Clin Orthop Relat Res*. 2001; 391(Suppl):S208–S218.
34. Pauli C, Grogan SP, Patil S, Otsuki S, Hasegawa A, Koziol J, Lotz MK, D’Lima DD. Macroscopic and histopathologic analysis of human knee menisci in aging and osteoarthritis. *Osteoarthritis Cartilage*. 2011; 19:1132–1141. [PubMed: 21683797]
35. Diaz-Romero J, Gaillard JP, Grogan SP, Nestic D, Trub T, Mainil-Varlet P. Immunophenotypic analysis of human articular chondrocytes: Changes in surface markers associated with cell expansion in monolayer culture. *J Cell Physiol*. 2005; 202:731–742. [PubMed: 15389573]
36. Boxall SA, Jones E. Markers for characterization of bone marrow multipotential stromal cells. *Stem Cells Int*. 2012; 2012:975871. [PubMed: 22666272]
37. Lin CS, Xin ZC, Dai J, Lue TF. Commonly used mesenchymal stem cell markers and tracking labels: Limitations and challenges. *Histol Histopathol*. 2013; 28:1109–1116. [PubMed: 23588700]
38. Barker TH, Hagood JS. Getting a grip on thy-1 signaling. *Biochim Biophys Acta*. 2009; 1793:921–923. [PubMed: 19007822]
39. Leyton L, Hagood JS. Thy-1 modulates neurological cell-cell and cell-matrix interactions through multiple molecular interactions. *Adv Neurobiol*. 2014; 8:3–20. [PubMed: 25300130]
40. Rege TA, Hagood JS. Thy-1, a versatile modulator of signaling affecting cellular adhesion, proliferation, survival, and cytokine/growth factor responses. *Biochim Biophys Acta*. 2006; 1763:991–999. [PubMed: 16996153]
41. Brunn GJ, Bungum MK, Johnson GB, Platt JL. Conditional signaling by toll-like receptor 4. *FASEB J*. 2005; 19:872–874. [PubMed: 15738005]
42. He J, Xiao Z, Chen X, Chen M, Fang L, Yang M, Lv Q, Li Y, Li G, Hu J, Xie X. The expression of functional toll-like receptor 4 is associated with proliferation and maintenance of stem cell phenotype in endothelial progenitor cells (epcs). *J Cell Biochem*. 2010; 111:179–186. [PubMed: 20506307]
43. Pevsner-Fischer M, Morad V, Cohen-Sfady M, Rousso-Noori L, Zanin-Zhorov A, Cohen S, Cohen IR, Zipori D. Toll-like receptors and their ligands control mesenchymal stem cell functions. *Blood*. 2007; 109:1422–1432. [PubMed: 17038530]
44. Humphries JD, Byron A, Humphries MJ. Integrin ligands at a glance. *J Cell Sci*. 2006; 119:3901–3903. [PubMed: 16988024]
45. Byron A, Morgan MR, Humphries MJ. Adhesion signalling complexes. *Curr Biol*. 2010; 20:R1063–R1067. [PubMed: 21172621]

46. Geiger B, Bershadsky A, Pankov R, Yamada KM. Transmembrane crosstalk between the extracellular matrix--cytoskeleton crosstalk. *Nat Rev Mol Cell Biol.* 2001; 2:793–805. [PubMed: 11715046]
47. Harburger DS, Calderwood DA. Integrin signalling at a glance. *J Cell Sci.* 2009; 122:159–163. [PubMed: 19118207]
48. Parsons JT, Horwitz AR, Schwartz MA. Cell adhesion: Integrating cytoskeletal dynamics and cellular tension. *Nat Rev Mol Cell Biol.* 2010; 11:633–643. [PubMed: 20729930]
49. Woods A, Wang G, Beier F. Regulation of chondrocyte differentiation by the actin cytoskeleton and adhesive interactions. *J Cell Physiol.* 2007; 213:1–8. [PubMed: 17492773]
50. Boudreau NJ, Jones PL. Extracellular matrix and integrin signalling: The shape of things to come. *Biochem J.* 1999; 339(Pt 3):481–488. [PubMed: 10215583]
51. Wixler V, Geerts D, Laplantine E, Westhoff D, Smyth N, Aumailley M, Sonnenberg A, Paulsson M. The lim-only protein dral/fhl2 binds to the cytoplasmic domain of several alpha and beta integrin chains and is recruited to adhesion complexes. *J Biol Chem.* 2000; 275:33669–33678. [PubMed: 10906324]
52. Horejs CM, Serio A, Purvis A, Gormley AJ, Bertazzo S, Poliniewicz A, Wang AJ, DiMaggio P, Hohenester E, Stevens MM. Biologically-active laminin-111 fragment that modulates the epithelial-to-mesenchymal transition in embryonic stem cells. *Proc Natl Acad Sci U S A.* 2014; 111:5908–5913. [PubMed: 24706882]
53. Margadant C, Monsuur HN, Norman JC, Sonnenberg A. Mechanisms of integrin activation and trafficking. *Curr Opin Cell Biol.* 2011; 23:607–614. [PubMed: 21924601]
54. Wu C, Chung AE, McDonald JA. A novel role for alpha 3 beta 1 integrins in extracellular matrix assembly. *J Cell Sci.* 1995; 108(Pt 6):2511–2523. [PubMed: 7673365]
55. Hirao M, Tamai N, Tsumaki N, Yoshikawa H, Myoui A. Oxygen tension regulates chondrocyte differentiation and function during endochondral ossification. *J Biol Chem.* 2006; 281:31079–31092. [PubMed: 16905540]
56. Huang W, Zhou X, Lefebvre V, de Crombrughe B. Phosphorylation of sox9 by cyclic amp-dependent protein kinase a enhances sox9's ability to transactivate a col2a1 chondrocyte-specific enhancer. *Mol Cell Biol.* 2000; 20:4149–4158. [PubMed: 10805756]
57. Malda J, van Blitterswijk CA, van Geffen M, Martens DE, Tramper J, Riesle J. Low oxygen tension stimulates the redifferentiation of dedifferentiated adult human nasal chondrocytes. *Osteoarthritis Cartilage.* 2004; 12:306–313. [PubMed: 15023382]
58. Aldinucci D, Poletto D, Lorenzon D, Nanni P, Degan M, Olivo K, Rapana B, Pinto A, Gattei V. Cd26 expression correlates with a reduced sensitivity to 2'-deoxycoformycin-induced growth inhibition and apoptosis in t-cell leukemia/lymphomas. *Clin Cancer Res.* 2004; 10:508–520. [PubMed: 14760072]
59. Kameoka J, Ichinohasama R, Inoue H, Yamamoto J, Yokoyama H, Tomiya Y, Yamada M, Ishizawa K, Harigae H, Sawai T, Sasaki T. Cd26, together with cell surface adenosine deaminase, is selectively expressed on alk-positive, but not on alk-negative, anaplastic large cell lymphoma and hodgkin's lymphoma. *Leuk Lymphoma.* 2006; 47:2181–2188. [PubMed: 17071493]
60. Hashikawa T, Hooker SW, Maj JG, Knott-Craig CJ, Takedachi M, Murakami S, Thompson LF. Regulation of adenosine receptor engagement by ecto-adenosine deaminase. *FASEB J.* 2004; 18:131–133. [PubMed: 14630704]
61. Holler N, Zaru R, Micheau O, Thome M, Attinger A, Valitutti S, Bodmer JL, Schneider P, Seed B, Tschoep J. Fas triggers an alternative, caspase-8-independent cell death pathway using the kinase rip as effector molecule. *Nat Immunol.* 2000; 1:489–495. [PubMed: 11101870]
62. Yurchenko M, Shlapatska LM, Sidorenko SP. The multilevel regulation of cd95 signaling outcome. *Exp Oncol.* 2012; 34:153–159. [PubMed: 23069999]
63. Aggarwal BB, Singh S, LaPushin R, Totpal K. Fas antigen signals proliferation of normal human diploid fibroblast and its mechanism is different from tumor necrosis factor receptor. *FEBS Lett.* 1995; 364:5–8. [PubMed: 7538467]
64. Jelaska A, Korn JH. Anti-fas induces apoptosis and proliferation in human dermal fibroblasts: Differences between foreskin and adult fibroblasts. *J Cell Physiol.* 1998; 175:19–29. [PubMed: 9491777]

65. Reinehr R, Sommerfeld A, Haussinger D. Cd95 ligand is a proliferative and antiapoptotic signal in quiescent hepatic stellate cells. *Gastroenterology*. 2008; 134:1494–1506. [PubMed: 18471522]
66. Desbarats J, Birge RB, Mimouni-Rongy M, Weinstein DE, Palerme JS, Newell MK. Fas engagement induces neurite growth through erk activation and p35 upregulation. *Nat Cell Biol*. 2003; 5:118–125. [PubMed: 12545171]
67. Knight JC, Scharf EL, Mao-Draayer Y. Fas activation increases neural progenitor cell survival. *J Neurosci Res*. 2010; 88:746–757. [PubMed: 19830835]
68. Billing AM, Ben Hamidane H, Dib SS, Cotton RJ, Bhagwat AM, Kumar P, Hayat S, Yousri NA, Goswami N, Suhre K, Rafii A, Graumann J. Comprehensive transcriptomic and proteomic characterization of human mesenchymal stem cells reveals source specific cellular markers. *Sci Rep*. 2016; 6:21507. [PubMed: 26857143]

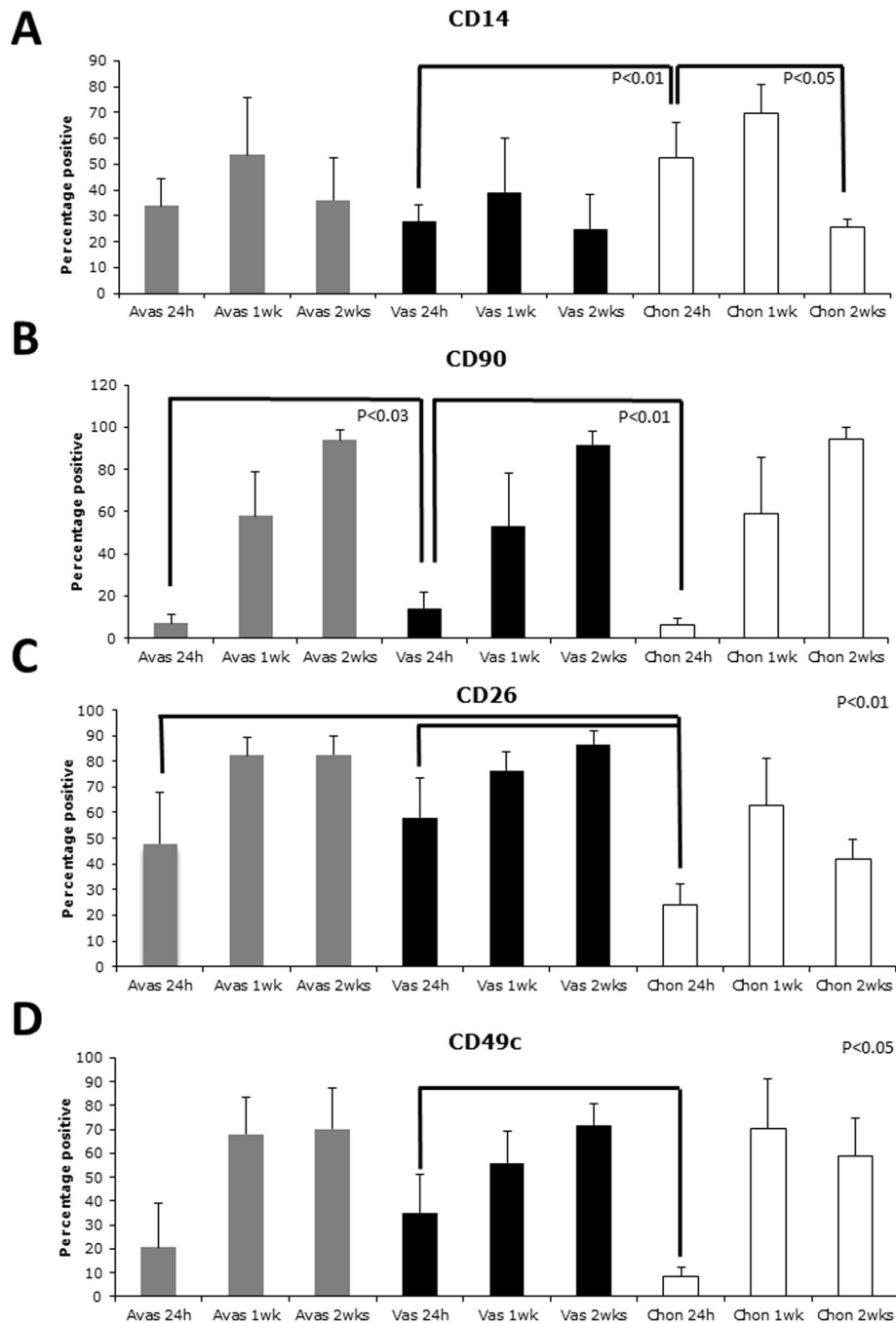


Figure 1. Surface molecule profiles (percentage positive) over time in culture on cells derived from either human avascular (Avas), vascular (Vas) meniscus tissue, or from human articular cartilage (Chon). **A.** CD14 levels did not significantly change on meniscus cells. A significant reduction on chondrocytes noted by 2 weeks in monolayer culture. **B.** Vascular-derived meniscus cells possessed significantly higher levels of CD90/THY-1 compared to the avascular-derived meniscus cells (24 h). **C.** A significantly higher percentage of CD26 positive cells from meniscus was detected in early culture (24 h). **D.** Significantly higher

percentage alpha 3 integrin (CD49c) was detected on cells isolated from the vascular region of meniscus compared to chondrocytes at 24 h.

Author Manuscript

Author Manuscript

Author Manuscript

Author Manuscript

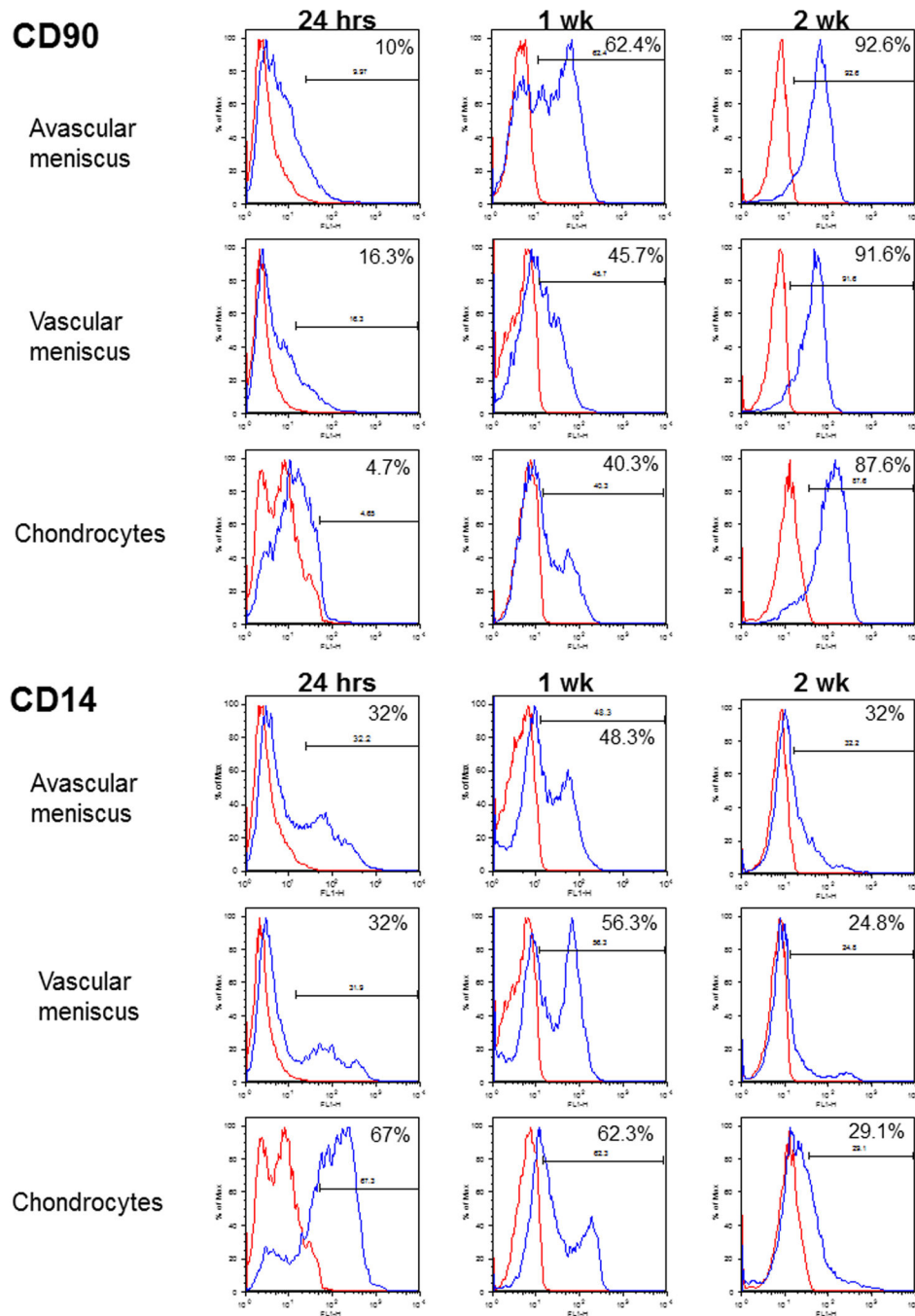


Figure 2. Representative percentage positive histograms for CD90 and CD14 for human avascular and vascular meniscus cells and in chondrocytes at 24 h, 1 week, and 2 weeks in monolayer culture.

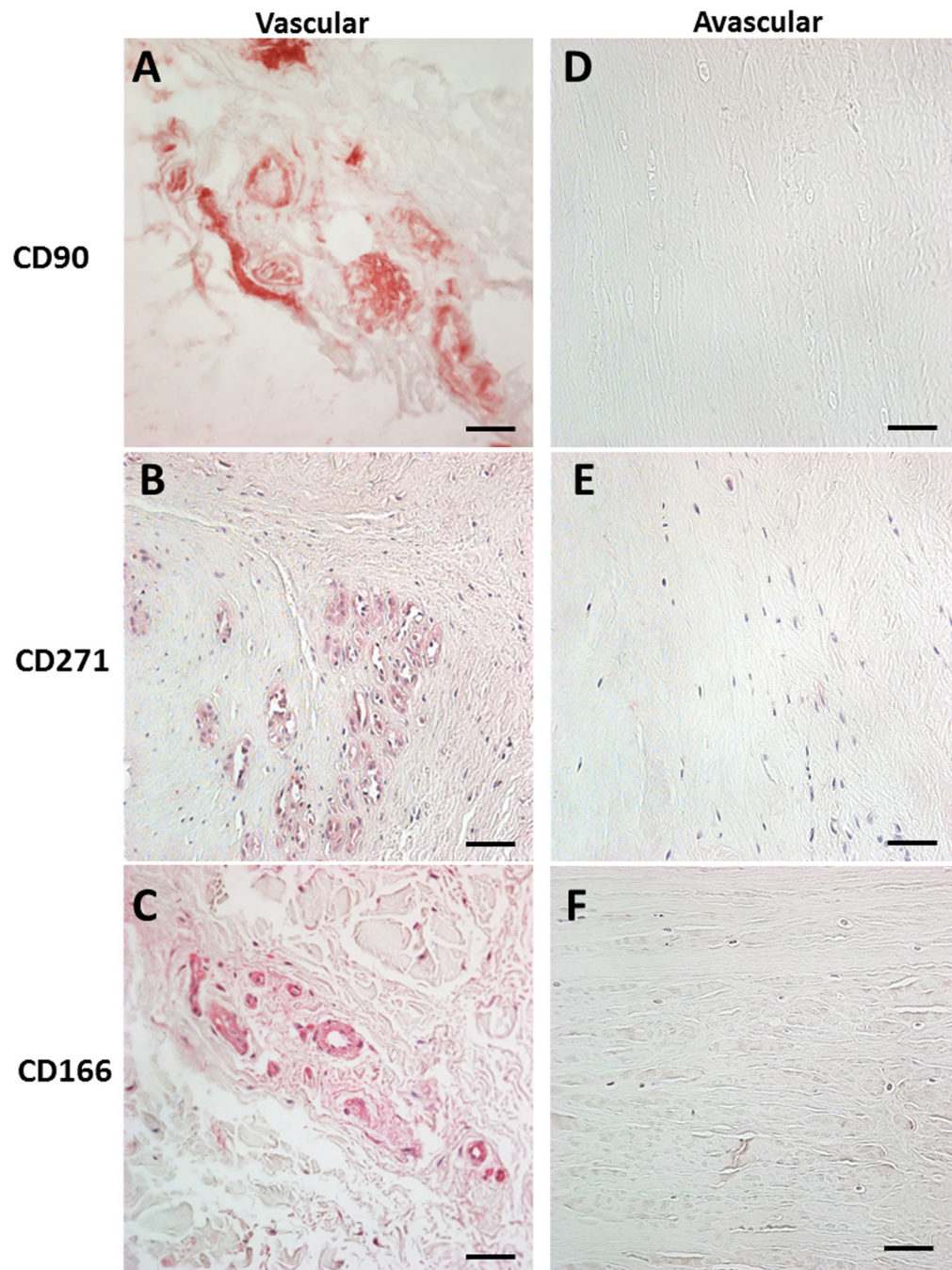


Figure 3. Immunohistochemistry of the vascular meniscus tissue region for multiple progenitor markers. Positive signals are associated with blood vessels indicating the presence of pericytes. No positive signals were seen in the avascular regions, with the exception of the surface of the meniscus spanning all regions (see Figure 4). **A.** CD90 / THY-1 in the vascular region. **B.** CD271 / LNGFR in the vascular region. **C.** CD166 / ALCAM in the vascular region. **D.** CD90 / THY-1 in the avascular region. **E.** CD271 / LNGFR in the

avascular region. **F.** CD166 /ALCAM in the avascular region. All images 40x magnification (scale bar 50 μ m).

Author Manuscript

Author Manuscript

Author Manuscript

Author Manuscript

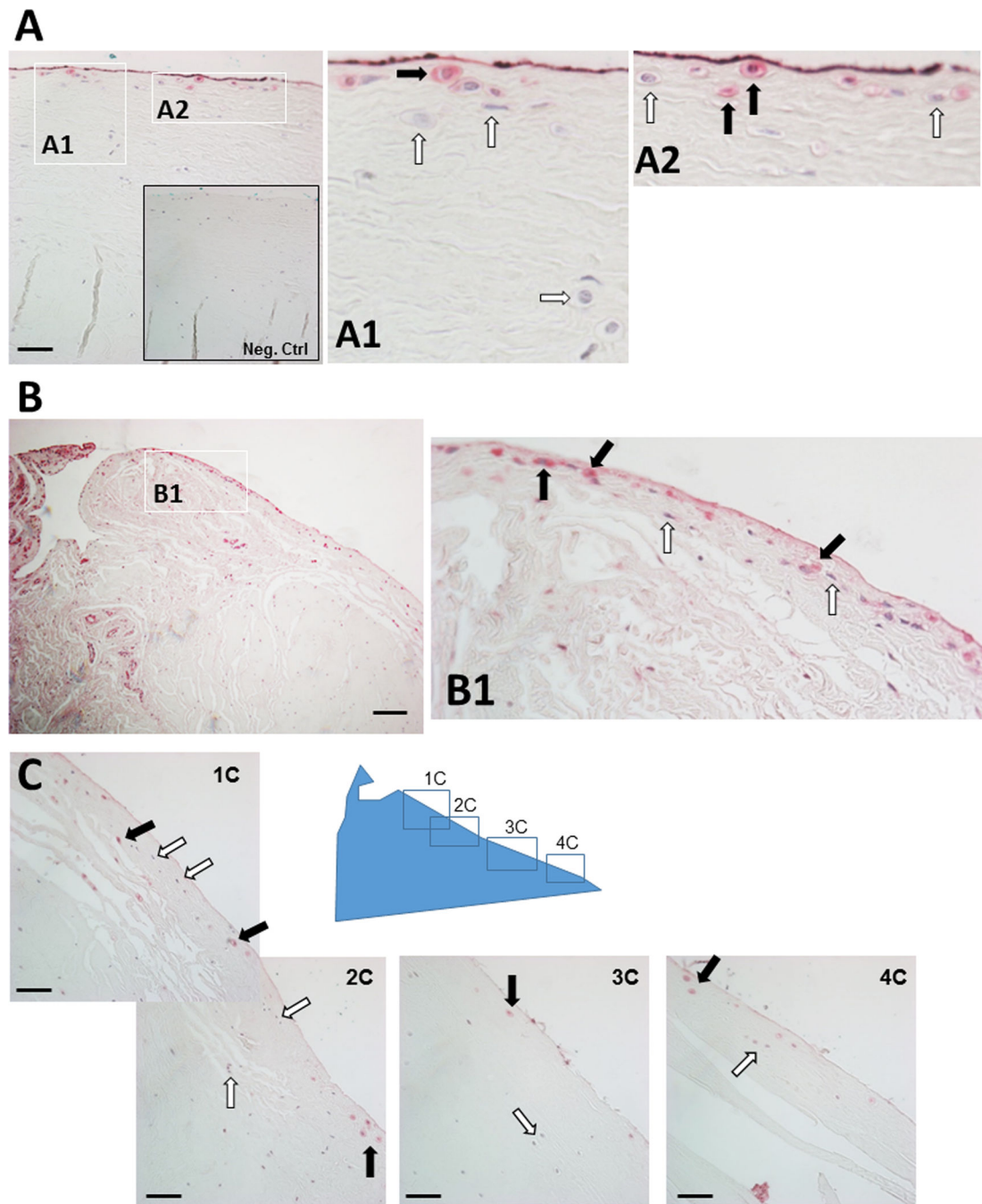


Figure 4. Immunohistochemistry of human menisci showing surface cell subpopulations positive for CD166 / ALCAM spanning the vascular and avascular regions. **A.** CD166 positive populations (40x; scale bar 50 μ m) with insets **1A** and **2A** showing positive and negative stains for CD166. Inset showing negative control (Neg. Ctrl). **B.** Vascular region with synovial-like tissue highly positive for CD166 (10x; scale bar 100 μ m). Inset: **B1** showing CD166 positive and negative cells. **C.** Series of surface images spanning the vascular and

avascular regions (40x; scale bar 50 μm). **Key:** Black arrows = positive for CD166 and white arrows = negative.

Author Manuscript

Author Manuscript

Author Manuscript

Author Manuscript

Table 1

Overview of percentage positive signal for each surface molecule monitored in avascular and vascular region meniscus cells and chondrocytes in monolayer culture after 24 h, 7 days, and 14 days in monolayer culture.

Surface molecule	Avas 24 h	Avas 1 wk	Avas 2 wks	Vas 24 h	Vas 1 wk	Vas 2 wks	Chon 24 h	Chon 1 wk	Chon 2 wks
CD14	33.9 ± 10.5	53.6 ± 22.4	36.2 ± 16.2	27.9 ± 6.4	39.2 ± 20.9	25.0 ± 13.1	52.4 ± 14.0	69.9 ± 10.7	25.5 ± 3.3 ^a
CD26	48.0 ± 19.7	82.3 ± 7.3	82.5 ± 7.3 ^c	58.0 ± 15.7	76.3 ± 7.6	86.5 ± 5.2 ^c	24.1 ± 8.2 ^b	62.6 ± 18.4	41.9 ± 7.5
CD44	78.6 ± 16.6	95.2 ± 5.3	99.2 ± 0.8 ^c	77.5 ± 14.8	90.9 ± 6.7	99.0 ± 1.0 ^c	84.1 ± 13.7	98.8 ± 1.0	98.3 ± 1.1
CD49a	27.8 ± 18.9	60.2 ± 18.6	61.2 ± 22.9 ^c	38.7 ± 19.7	59.5 ± 10.2	58.0 ± 21.3 ^c	39.2 ± 3.8	71.8 ± 14.4	29.5 ± 14.4
CD49c	20.8 ± 18.2	68.1 ± 15.4	70.2 ± 17.3 ^c	35.2 ± 16.0 ^d	55.9 ± 16.6	71.9 ± 9.1 ^c	8.2 ± 4.2	70.6 ± 20.5	58.7 ± 15.9 ^c
CD49e	43.1 ± 26.0	83.4 ± 13.0	94.4 ± 5.3 ^c	48.2 ± 25.3	76.7 ± 29.5	92.1 ± 10.1 ^c	62.0 ± 23.3	92.8 ± 0.1	95.6 ± 4.0 ^c
CD49f	0.7 ± 0.2	2.4 ± 1.7	10.6 ± 6.8 ^c	0.8 ± 0.32 ^d	2.3 ± 1.3	6.6 ± 3.6 ^c	1.2 ± 0.1	3.3 ± 3.0	3.3 ± 2.6
CD54	63.8 ± 21.8	84.8 ± 13.3	90.9 ± 6.7 ^c	61.5 ± 16.1	80.2 ± 11.0	87.0 ± 7.5 ^c	68.6 ± 6.0	90.5 ± 4.5	87.9 ± 6.0 ^c
CD90	7.2 ± 3.9	57.8 ± 21.3	93.9 ± 5.1 ^c	14.3 ± 7.6 ^e	53.0 ± 25.2	91.7 ± 6.4 ^c	6.1 ± 3.4	59.2 ± 26.7	94.1 ± 5.6 ^c
CD95	1.1 ± 0.6	14.3 ± 9.6	53.4 ± 16.9 ^c	2.7 ± 4.0	8.0 ± 11.1	56.6 ± 25.1 ^c	0.9 ± 0.6	11.8 ± 7.1	40.9 ± 10.7 ^c
CD105	0.5 ± 0.2	0.4 ± 0.4	0.6 ± 0.8	0.6 ± 0.3	0.2 ± 0.3	0.2 ± 0.1	0.4 ± 0.1	0.2 ± 0.2	3.1 ± 2.6
CD106	33.2 ± 17.8	76.7 ± 13.0	86.0 ± 10.3 ^c	30.8 ± 17.4	64.0 ± 15.0	83.0 ± 12.3 ^c	23.6 ± 24.0	89.6 ± 5.9	89.2 ± 7.0 ^c
CD140a	38.2 ± 22.6	81.1 ± 17.9	90.8 ± 9.2 ^c	44.5 ± 24.5	75.8 ± 12.6	80.0 ± 8.1 ^c	27.2 ± 15.5	88.7 ± 9.7	79.8 ± 17.2 ^c
CD151	48.3 ± 30.7	79.8 ± 12.5	93.4 ± 5.4 ^c	53.2 ± 23.6	74.5 ± 18.7	88.2 ± 9.7 ^c	40.7 ± 32.9	79.0 ± 19.7	92.9 ± 6.2 ^c
CD166	2.2 ± 1.8	34.0 ± 25.6	57.5 ± 7.7 ^c	5.2 ± 6.8	27.8 ± 13.7	62.6 ± 13.1 ^c	2.2 ± 0.5	34.0 ± 21.5	43.3 ± 21.5 ^c
CD271	0.9 ± 0.5	1.2 ± 1.3	1.3 ± 0.7	2.5 ± 3.0	1.7 ± 1.8	1.3 ± 0.6	1.3 ± 0.4	0.9 ± 0.1	0.9 ± 0.6

Note: All significant values $P < 0.05$;

^a sig. decrease in % positive signal between 24 h and 2 wk;

^b sig. lower in 24 h Chon 24 h compared to Vas and Avas;

^c sig increase in % positive signal between 24 h and 2 wk;

^d sig higher % positive signal in 24 h Vas compared to 24 h Chon;

^e sig higher % positive signal in 24 h Vas compared to 24 h Avas and 24 h Chon;

Table 2

Fold change in percentage positive signal for each cell source relative to 24 h.

	avasc-1w	avasc-2w	vasc-1w	vasc-2w	chond-1w	chond-2w
CD14	1.6	1.1	1.4	0.9	1.3	-2.1
CD26	1.7	1.7	1.3	1.5	2.6	1.7
CD44	1.2	1.3	1.1	1.0	1.2	1.1
CD49a	2.2	2.2	1.5	1.5	1.8	0.8
CD49c	3.3	3.4	1.6	2.0	8.6	7.1
CD49e	1.9	2.2	1.6	1.9	1.5	1.5
CD49f	3.4	14.7	2.8	8.1	2.7	2.6
CD54	1.3	1.4	1.3	1.4	1.3	1.3
CD90	7.9	12.9	3.7	6.4	9.7	15.5
CD95	12.6	47.1	3.0	21.3	13.8	47.9
CD105*	-	-	-	-	-	-
CD106	2.3	2.6	2.1	2.7	3.8	3.8
CD140a	2.1	2.4	1.7	2.0	3.3	2.9
CD151	1.7	1.9	1.4	1.7	1.9	2.3
CD166	15.7	26.6	5.3	12.0	15.6	19.9
CD271*	-	-	-1.4	-2.0	-	-

Key: Numbers in **bold** P < 0.05.

* At or below background signal.

Table 3

Mean Fluorescence Intensity (MFI) for each cell source relative to 24 h.

	avasc-1w	avasc-2w	vasc-1w	vasc-2w	chondros-1w	chondros-2w
CD14	1.4	1.0	0.9	1.0	1.0	-2.0
CD26	1.4	1.3	0.9	1.0	1.0	1.1
CD44	2.9	3.5	2.1	3.0	3.4	2.2
CD49a	1.3	1.2	1.0	1.0	1.2	0.8
CD49c	1.4	1.4	1.0	1.1	1.4	1.2
CD49e	1.9	2.4	1.5	1.7	1.6	1.7
CD49f	1.3	1.2	1.4	1.3	1.0	1.2
CD54	1.4	1.5	1.0	0.9	1.2	1.2
CD90	2.0	3.0	1.2	1.8	2.3	3.8
CD95	1.2	1.3	1.0	1.4	1.0	1.2
CD105*	-	-	-	-	-	-
CD106	1.8	1.9	1.2	1.4	2.1	1.9
CD140a	2.0	2.3	1.5	1.9	2.1	1.8
CD151	1.7	2.2	1.2	1.7	1.6	2.1
CD166	1.4	1.6	1.4	1.5	1.3	1.4
CD271*	-	-	1.6	1.4	-	-

Key: Numbers in **bold** indicate $P < 0.05$.

* At or below background signal.